CHEMISTRY
AN ASIAN JOURNAL
www.chemasianj.org

Accepted Article

Title: Single-walled Carbon Nanotube Based Ultrafast High Capacity Al-ion Battery

Authors: Preeti Bhauriyal, Arup Mahata, and Biswarup Pathak

To be cited as: *Chem. Asian J.* 10.1002/asia.201700570

Link to VoR: http://dx.doi.org/10.1002/asia.201700570

A Journal of

ACES Asian Chemical Editorial Society

A sister journal of Angewandte Chemie and Chemistry – A European Journal

WILEY-VCH

10.1002/asia.201700570

A Computational Study of Single-walled Carbon Nanotube Based Ultrafast High Capacity Aluminium Battery

Preeti Bhauriyal,[†] Arup Mahata,[†] Biswarup Pathak, [†,#,*]

[†]Discipline of Chemistry, and [#] Discipline of Metallurgy Engineering and Materials Science, Indian Institute of Technology (IIT) Indore, Indore, M.P. 453552, India

Email: biswarup@iiti.ac.in

Abstract

Exploring a suitable electrode material is a fundamental step in the direction of the development of aluminium battery for enhanced performance. In this work, we have explored the feasibility of single-walled carbon nanotubes (SWNTs) as a cathode material for aluminium batteries using the density functional theory calculations. Carbon nanotubes with the hollow structures and large surface area overcome the difficulty of activating the opening of interlayer spaces as observed in graphite electrode during the first intercalation cycle. Our results show that $AlCl_4$ binds strongly with the SWNT resulting into energetically and thermally stable $AlCl_4$ adsorbed SWNT system. The diffusion calculation shows that the SWNT system allows ultrafast diffusion of $AlCl_4$ with a more favourable inner surface diffusion over outer surface diffusion. Our charge density difference and Bader atomic charge analysis confirm the oxidation of SWNT on $AlCl_4$ adsorption, showing a similar behaviour like previously studied graphite cathode. The average open-circuit voltage and $AlCl_4$ storage capacity increases with increasing SWNT diameter and can be as high as 1.96 V and 275 mAh/g, respectively in (25,25) SWNT compared to graphite

(70 mAh/g). All of these properties show that SWNTs are potential cathode material for high-performance aluminium batteries and should be explored further.

Keywords: Aluminium battery, Single-walled carbon nanotube, Density functional theory, Specific capacity, Average open-circuit voltage

Introduction

Energy storage is an ever growing technology that satisfies the world's power need from portable electronic devices to electric vehicles and large-scale power grid systems [1, 2]. Among the different types of energy storage systems, secondary batteries have received remarkable attention because of their great advantages of compact size and high efficiency [3-5]. Secondary batteries also known as rechargeable batteries or storage battery which are potentially consist of reversible cell reactions that allow them to recharge their cell potential through the work done by passing currents of electricity [3-5]. A promising way of achieving these goals is the modification of metal-ion batteries that frames the efficiency and energy storage capacity of the secondary batteries [6-8]. The world's research interest is moving from the traditional Li-ion batteries, which are associated with the limitations such as safety, production cost, and reactivity [9-11] to the newly emerging field of multivalent batteries (Mg [12-14], Zn [15-16], Al [17-26]) due to their large natural resources, high energy density, and capacity. Among these developing technologies, aluminium batteries have distinctive advantages because its three electron redox couple provides high theoretical specific capacity 2.89 Ahg-1 and volumetric charge storage capacity 8.0 Ah/cm^3 [19, 20]. Many electrode materials have been studied for aluminium batteries which have essentially played an important role in increasing the efficiency of these batteries as well as opening new doors for further research attentive [17-18, 20-23, 26]. An aluminium battery that is comprised of three-dimensional graphitic-foam cathode graphite has

attracted a worldwide attention due to its ultrafast charging rate and involvement of intercalation/deintercalation of $AlCl_4$ anions during charging/discharging respectively [27]. Soon after that, with the help of dispersion corrected DFT study, we predicted that not only the graphite foam, but the natural graphite can also be used as the cathode material in aluminium batteries, which intercalates tetrahedral $AlCl_4$ forming different stages with an average voltage of 2.3 V [28]. At the same time, some recent experimental studies on advanced rechargeable aluminium battery have also produced the similar results with natural graphite [29-32]. However, many experimental studies on anion intercalation and the theoretical study conducted by us into graphite electrode have shown that the very first intercalation step (cycle) differs from the other successive steps because it involves kind of activation of partially closed interlayer spaces of graphite layers during the first intercalation of the anion, which results into lower discharge capacities [30, 33, 34]. Thus it becomes important to look for other electrode materials which can overcome the interlayer gallery opening difficulty in the first intercalation step in graphite like layered materials [28, 35] and increase the battery performance.

Among the various carbon allotropes, carbon nanotubes (CNTs) based materials can be promising for the first intercalation step of aluminium battery. CNTs have been a subject of interest to chemists and physicists ever since discovered by Iijima in 1991 [36]. The superior electronic and structural properties of carbon nanotubes (CNTs) have significantly motivated the world's interest for the building blocks in future nanodevices. The literature surveys show that CNTs are considerably feasible for high storage capacity than their corresponding graphite counterparts with hollow structures which possess large surface area, more guest binding sites and easy transmission [37-47]. In addition, the tubular structure of CNTs acts as a host for various molecules and atoms that can be encapsulated inside CNTs and the hollow interior

cavities provide large space for mitigating the strain associated with the structural change due to repeated guest intercalation/deintercalation, increasing the cycle life of batteries [40, 48-49]. Very recently, an aluminium asymmetric capacitor utilizing multi-walled carbon nanotube and Al metal anode is proposed which also involves adsorption/desorption and intercalation/deintercalation of $AlCl_4$ during charging/discharging of the capacitor [50]. However, the feasibility of carbon nanotubes for aluminium batteries is still unexplored.

In this present paper, we have studied the great potential of the armchair single-walled carbon nanotubes (SWNTs) to be the high capacity cathode materials for aluminium batteries. The first principles calculations are performed for the systematic study of $AlCl_4$ adsorption on SWNTs with varying diameters and locating different adsorption positions on each tube to evaluate the adsorption behaviour of the system and structural and thermal stability. The density of states, charge density difference [51-52], and Bader charge [53-59] calculations are carried out to examine the extent of interaction between adsorbed $AlCl_4$ and the tube. We have also done the detailed investigation to understand the diffusion pathways for $AlCl_4$ diffusion in SWNT. Furthermore, we have also discussed the effect of varying SWNT diameters on the average open-circuit voltage and specific capacity of SWNT based aluminium batteries. Finally, we conclude that the results are promising and promote a potential electrode material for aluminium batteries.

Results and Discussions

$AlCl_4$ Adsorption, Stability and Electronic Properties

Depending on the way the graphene is rolled, different chiralities are possible which are generally identified by their chiral vector (n,m). The SWNT is metallic, when the difference between two components of the chiral vector (n,m) is a multiple of 3, otherwise it is

semiconducting. The metallic and semiconducting SWNTs have different electrochemical properties including the storage property [60]. It is well accepted by both theoretical and experimental studies that storage capacity of metallic single-walled CNTs is about 5 times greater than that of the semiconducting ones [60]. Therefore, based on their finding we have carried out our study using armchair metallic SWNTs [61, 62]. Firstly, we have taken (10,10) SWNT system as an example to study the adsorption behaviour, and electronic properties of $AlCl_4$ adsorbed SWNT. The (10,10) SWNT is experimentally synthesized and has been immensely studied for Li-ion batteries [37, 63-64].

Firstly, we start by examining the most stable geometry of $AlCl_4$ inside the nanotube, whether it is planar or tetrahedral. We obtained that the tetrahedral geometry of $AlCl_4$ is stable in SWNT and there is a negligible change in the geometry, Al-Cl bond lengths and Cl-Al-Cl bond angle of $AlCl_4$. Also, there is very negligible structural distortion of SWNT after $AlCl_4$ adsorption. However, on examining the system stability with the planar $AlCl_4$ molecule, it is observed that the planar geometry of $AlCl_4$ changes to tetrahedral geometry after optimization. The stability of tetrahedral geometry over planar is in agreement with our gas phase calculations, where the tetrahedral $AlCl_4$ molecule is 0.88 eV more stable than the planar $AlCl_4$ and it is also supported by our earlier report for $AlCl_4$ intercalation in graphite [28]. The structural change of $AlCl_4$ from planar to tetrahedral in SWNT after adsorption justifies the energetic results that the tetrahedral $AlCl_4$ is more favourable in SWNT.

Next, we have studied the most stable adsorption site of $AlCl_4$ on the inner and outer surface of SWNT. Unlike the intercalation of $AlCl_4$ in graphite cathode, here the adsorption of $AlCl_4$ occurs on the SWNT surface and this concept of $AlCl_4$ adsorption has also been studied in the previous experimental reports [20, 65]. We have set three orientations of $AlCl_4$ adsorption as shown in

10.1002/asia.201700570

Figure 1a-c. Further, we have considered five adsorption sites (Figure 1d-h): (i) hollow site 1 (H-1), (ii) hollow site 2 (H-2), (iii) top site 1 (T-1), (iv) top site 2 (T-2), and (v) bridge site (B). The binding of $AlCl_4$ on SWNT is studied by calculating the adsorption energy E_{ad} using the equation,

$$E_{ad} = (E_{SWNT+AlCl_4} - E_{SWNT} - E_{AlCl_4})$$

where, $E_{SWNT+AlCl_4}$ and E_{SWNT} and E_{AlCl_4} are the total energies of SWNT with $AlCl_4$, SWNT, and one $AlCl_4$ molecule in the box, respectively. The negative E_{ad} value means favourable adsorption. Our relative energetic study (Table S1, Supporting Information) shows that $AlCl_4$ prefers to be adsorbed through 3-Cl orientation (three Cl atoms facing the surface) as shown in Figure 1c. This orientation is favourable for $AlCl_4$ adsorption on the inner and outer surfaces. The results show that the H-1 site is the most stable site for $AlCl_4$ adsorption. Similarly, site choices are also observed for other metal ion and anions on SWNTs, graphite and their derivatives [63]. Figure S1 (Supporting Information) displays the binding energy variation as a function of adsorption height from the tube surface for both inner and outer surface $AlCl_4$ adsorption. Clearly, the adsorption is more favourable when $AlCl_4$ is located near the surface compared to the centre of the ring with the equilibrium C-Cl distance of about 3.40 Å from the inner surface and 3.46 Å from the outer surface.

10.1002/asia.201700570

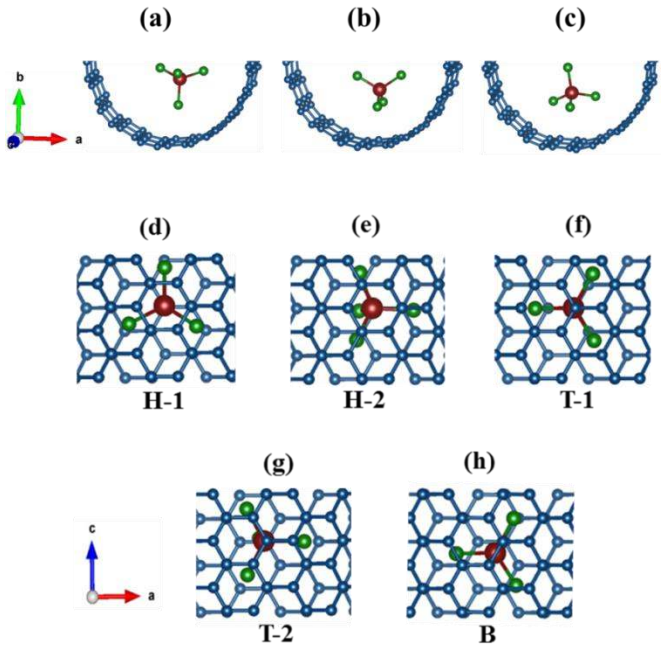

Figure 1: Top view of $AlCl_4$ orientations: (a) 1-Cl, (b) 2-Cl, (c) 3-Cl. Side view of the possible adsorption sites for $AlCl_4$ adsorption, (d) Hollow site (H-1), (e) Hollow site (H-2), (f) Top site (T-1), (g) Top site (T-2), (h) Bridge site (B).

To further understand the adsorption behaviour and nature of interactions between $AlCl_4$ and SWNTs, we have analysed the electronic properties like density of states and charge density difference calculations [51-52] (Figure 2). The armchair carbon nanotubes are metallic in nature with good electrical conductivity [61-63], which is a deciding factor for investigating the electrochemical properties. The total and projected density of states depicted in Figure 2 show that the tube remains metallic on adsorption of $AlCl_4$ on inner as well as on outer surfaces. We observe significant overlap between C_*2p* orbital and Cl_*3p* orbital in -2.5 to 0 eV energy range, indicating towards the interaction between adsorbed $AlCl_4$ and nanotube.

The previous experimental and theoretical reports on graphite electrode conclude that the $AlCl_4$ intercalation results in the oxidation of graphitic carbons with 1|e| charge transfer per $AlCl_4$

molecule intercalated [27, 28]. Similarly, to check the nature of bonding between $AlCl_4$ and nanotube, we have calculated the charge density difference, as expressed by the following formula [51-52],

$$\Delta\rho(r) = \rho_{SWNT+AlCl_4}(r) - \rho_{SWNT}(r) - \rho_{AlCl_4}(r)$$

where, $\rho_{SWNT+AlCl_4}(r)$, $\rho_{SWNT}(r)$, and $\rho_{AlCl_4}(r)$ are the charge densities of $AlCl_4$ adsorbed SWNT system, SWNT (without $AlCl_4$) and isolated $AlCl_4$ molecule adsorbed at the same position as in the total system. Figure 2b and 2d show the charge density difference of the $AlCl_4$ molecules adsorbed at the H-1 site on the inner and outer surfaces, respectively. There is a net gain of electronic charge around each Cl atom of $AlCl_4$ molecule and a net loss of electronic charge on neighbouring C atoms of SWNT surface, indicating the charge transfer from tube towards the Cl atoms of $AlCl_4$ molecule and oxidation of SWNT after $AlCl_4$ adsorption.

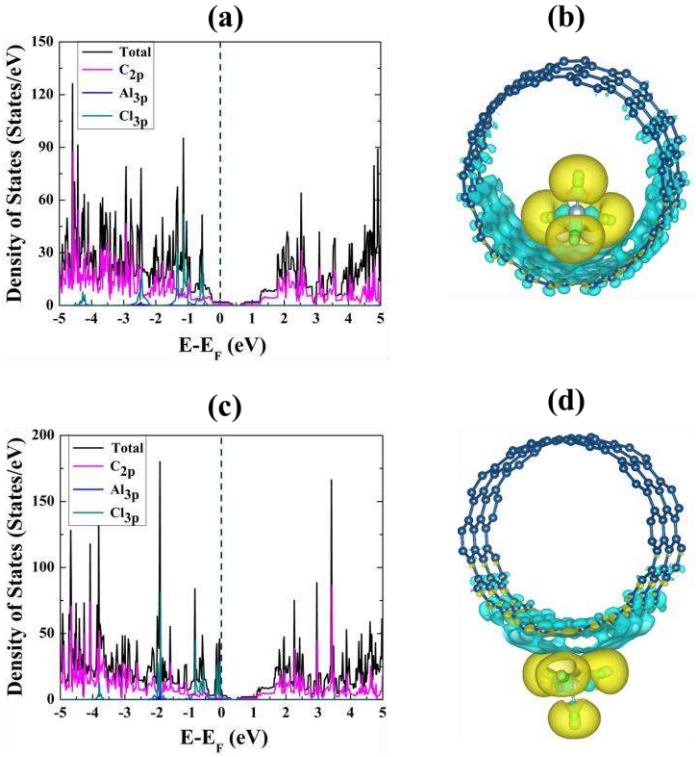

Figure 2: Density of states and charge density difference of the $AlCl_4$ adsorbed SWNT for (a-b) inner and (c-d) outer surface adsorption of $AlCl_4$. The Fermi energy is set to zero. Isosurface value is 0.0003; yellow and blue represent $\Delta\rho > 0$ and $\Delta\rho < 0$, respectively.

Next, we have performed the AIMD simulations to investigate the thermal stability of $AlCl_4$ adsorbed (10,10) SWNT using NVT ensemble and Nóse thermostat [66]. The analysis is carried out at a temperature range of 300-600 K with the time scale of 1 femtosecond for 5 picoseconds and the observed time evolution of total energy during the simulations is shown in Figure S2 (Supporting Information). The $AlCl_4$ adsorbed on the most stable H-1 adsorption site is considered for the calculations. For the simulation at 300 K temperature, the total energy value reaches the equilibrium very quickly (in 1 ps) and fluctuates near the equilibrium. The structure snapshots in Figure S2(a) show that no structural reconstruction of $AlCl_4$ and SWNT structures occurs at 300 K, however having a lateral shifting of $AlCl_4$ site position and slight distortion of SWNT structure. Furthermore, MD simulations are carried out at higher temperatures 400 K, 500 K and 600 K and the total energy shows larger fluctuations with increasing temperature of the NVT system. We observe that the tetrahedral geometry of $AlCl_4$ is preserved, but the orientation and position of $AlCl_4$ slightly changes from the optimized structure and for SWNT, the structural distortion is similar to lower temperature simulation result. Overall, we can conclude that the $AlCl_4$ intercalated SWNT system is stable even at higher temperatures and shows no structural reconstruction. The second important conclusion that can be inferred is about the rate capability of the battery as the $AlCl_4$ is not strongly bonded to one specific site (very small difference between the possible binding sites) and changes the relative position without changing the nature of chemical bonding with SWNT system. This can lead to lower diffusion barrier for $AlCl_4$

diffusion into SWNT system, providing ultrafast charging rate. Thus, we can also examine SWNT for aluminium battery, which can provide fast charging/discharging rate.

Next, we have evaluated the adsorption energies of $AlCl_4$ on the most stable H-1 site for different SWNTs (5,5), (6,6), (10,10), (15,15), (20,20) and (25,25) on the inner surface, the outer surface and at the centre of nanotubes as shown in Figure 3. The side views of single-walled SWNTs employed in our study are shown in Figure S3 (Supporting Information) with their respective diameters. In (5,5) SWNT, we observe that the only possible adsorption is on the outer surface with -1.82 eV adsorption energy because the diameter of SWNT (6.92 Å) is comparatively smaller to accommodate large sized $AlCl_4$ (5.28 Å) [67] in the inner cavity. However, both inner and outer surface adsorption patterns are stable for higher SWNTs. Our calculations show that the inner adsorption is very less favourable (-0.70 eV) as compared to the outer adsorption (-1.83 eV) in (6,6) SWNT. However, for larger SWNTs, the adsorption of $AlCl_4$ on the inner surface becomes more favourable. From Figure 3 and Table S2 (Supporting Information), it is clear that as the SWNT diameter increases, the adsorption at the centre of the tube decreases and the difference between inner and outer adsorption becomes less. Initially, for (10,10) SWNT, the inner surface adsorption energy is largest followed by the adsorption at the tube centre and outer surface adsorption. The inner surface adsorption becomes less favourable while the outer surface adsorption energy increases a little with the increase in diameter and becomes almost equal for (25,25). Similar trends have also been observed for other metal-ion adsorption and the reason for this behaviour is the flattening of the nanotube with increasing diameters that frames it to behave like a single sheet [63, 68]. All these results conclude that both the inner and outer surfaces are capable of storing $AlCl_4$ which can lead to high storage capacity for SWNTs.

10.1002/asia.201700570

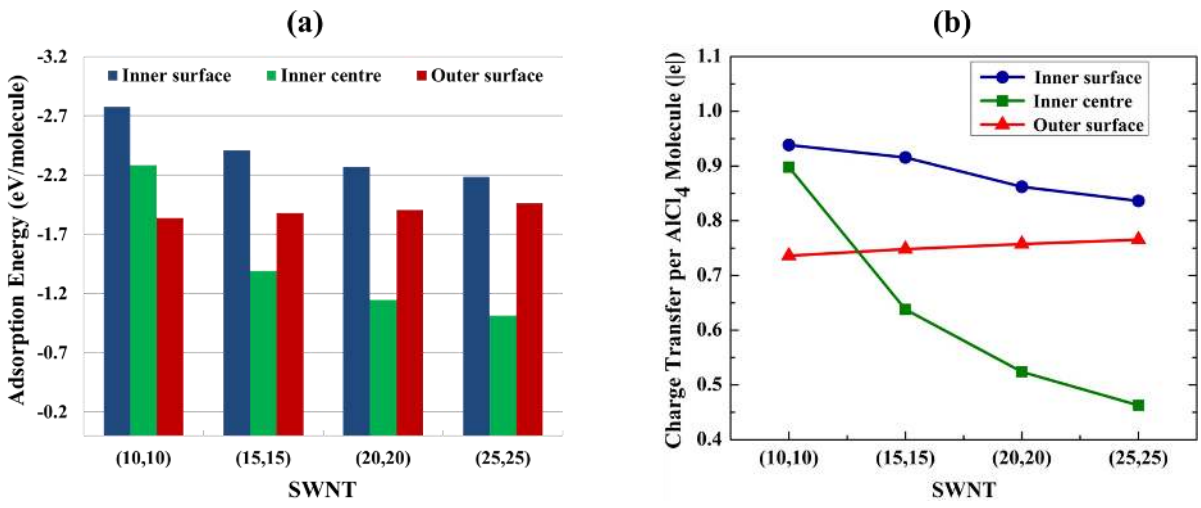

Figure 3: (a) Adsorption energies of $AlCl_4$ on the inner, outer surface and on the centre of the inner surface for different single walled SWNTs. (b) Charge transfer per $AlCl_4$ molecule for inner, outer surface and inner centre of different single walled SWNTs.

The Bader charge analysis [53-59] is performed for the quantitative estimation of the extent of charge transfer between $AlCl_4$ and the SWNTs. The net effective charges on each Cl atom of adsorbed $AlCl_4$ and nearest C atoms are examined for the (10,10), (15,15), (20,20) and (25,25) SWNTs for three adsorption possibilities (inner surface, outer surface and inner centre) and the calculated net charge transfer is given in Table S2 (Supporting Information). Further, Figure 3 shows the systematic variation with SWNT diameters and the results clearly indicate towards the electrochemical oxidation of SWNTs on $AlCl_4$ adsorption, thus we can say that the electrochemical behaviour of SWNTs will be similar to graphite [27-28], when being used as a cathode for aluminium batteries. The net charge transfer value from nearest C atoms to $AlCl_4$ is high when $AlCl_4$ adsorption is stronger at SWNT surface. The maximum charge transfer occurs in (10,10) SWNT, when the adsorption of $AlCl_4$ occurs on the inner surface because of the upmost interaction between $AlCl_4$ and the surface Carbons. The charge transfer for the inner

surface adsorption deceases with the increasing diameter of SWNTs, and the reverse order is observed for outer surface adsorption.

$AlCl_4$ Diffusion on (10, 10) SWNT Surface

Mobility of ions is an important factor for determining the rate performance of a particular battery at which the battery can be charged and discharged. In particular, a low diffusion barrier and high mobility are much desired to make a promising electrode material. Therefore, we have investigated the diffusion of $AlCl_4$ on both inner and outer surfaces of SWNT from its neighbouring equivalent sites. We have taken $1 \times 1 \times 6$ supercell of (10,10) SWNT to investigate the diffusion paths and diffusion barriers. Two different diffusion directions are considered as shown in Figure 4a. The associated energy barriers along these paths are calculated and the energy profiles are shown in Figure 4b-c. We find that the preferred diffusion pathways of $AlCl_4$ on inner and outer surfaces of SWNTs are quite energetically different. For inner surface diffusion, the preferable path is in the axial direction is path 1-2, showing a diffusion barrier of 0.003 eV, whereas the outside diffusion along the axis (path 1-3) possesses a barrier of 0.006 eV. The saddle point corresponds to a configuration where $AlCl_4$ is below (above) the C-C bridge site for inner (outer) surface diffusion. We observe that the diffusion of $AlCl_4$ inside the tube is more directional as compared to outer surface diffusion with the higher difference in diffusion barrier for path 1-2 selectivity. However, for outer surface diffusion, the difference in diffusion barriers along different pathways is less. On a flat graphite layer, these maximum energies (inside –outside) are equal because of structural symmetry. For the case of SWNTs, however, the asymmetry caused by curvature effect separates these maximum energies, giving rise to different diffusion barriers. The weakening of curvature effect of outer side saturates the diffusion barriers at the same value [68]. The second reason could be that we have only investigated an isolated

SWNT system and the contributions of interactions between adjacent tubes have not been taken. We would like to mention that the choices of diffusion direction on both inner and outer surfaces agree well with the Li-ion battery on SWNTs, however with smaller diffusion barriers (0.003 eV, 0.006 eV) as compared to diffusion barrier of Li-ion (0.046 eV, 0.147 eV) on SWNT [68]. Thus, we believe that the SWNTs with low diffusion barrier along with other desirable properties can ensure high rate performance for aluminium battery.

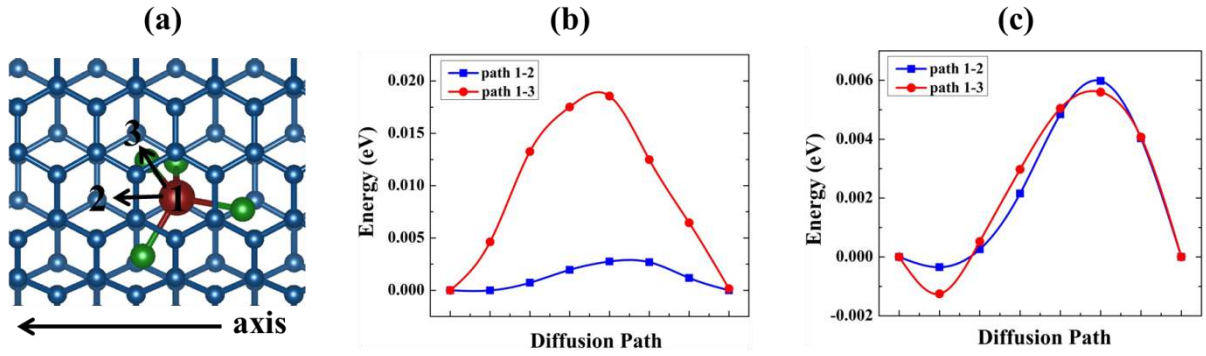

Figure 4: (a) Schematic representation of the top view of the considered diffusion paths. Corresponding diffusion barrier profiles for $AlCl_4$ on (10,10) SWNT (b) Inner surface and (c) Outer surface.

Open-Circuit Voltage and Storage Capacity

The standard chemical reaction involved in ionic liquid electrolyte based aluminium batteries can be described as follows,

Anode: $$Al + 7AlCl_4^- \rightleftharpoons 4Al_2Cl_7^- + 3e^-$$

Cathode: $$C_n[AlCl_4] + e^- \rightleftharpoons C_n + AlCl_4^-$$

The overall cell reaction can be represented with the given expression [20],

$$3[(AlCl_4)SWNT] + 4(EMI^+AlCl_4^-) + Al \leftrightarrow 3SWNT + 4(EMI^+Al_2Cl_7^-)$$

For x number of $AlCl_4$ adsorbed on SWNT the net reaction can be expressed as,

$$3/x[(AlCl_4)_xSWNT] + 4(EMI^+AlCl_4^-) + Al \leftrightarrow 3/xSWNT + 4(EMI^+Al_2Cl_7^-)$$

The cell voltage can be determined by the Nernst equation [69-70],

$$V = -\frac{\Delta G_{cell}}{zF}$$

where z and F are the number of valence electrons during the intercalation process and the Faraday constant, respectively; ΔG_{cell} is the change in Gibbs free energy for chemical reaction of aluminium battery, which can be approximated to the internal energy ($\Delta G_f = \Delta E + P\Delta V - T\Delta S$) at 0 K due to negligible contribution of entropy and volume effect on the cell voltage. Thus, the cell voltage can be calculated by computing the corresponding internal energy change as [28],

$$\Delta E = \{{}^3/_x E_{[(AlCl_4)_xSWNT]} + 4E_{[EMI^+AlCl_4^-]} + E_{Al}\} - \{{}^3/_x E_{SWNT} + 4E_{[EMI^+Al_2Cl_7^-]}\}$$

where $E_{[(AlCl_4)_xSWNT]}$, $E_{[EMI^+AlCl_4^-]}$ and $E_{[EMI^+Al_2Cl_7^-]}$ are the total energies of the $AlCl_4$ adsorbed SWNT system, $EMI^+AlCl_4^-$ and $EMI^+Al_2Cl_7^-$, respectively. E_{Al} is the total energy of a single Al atom in a bulk fcc structure and E_{SWNT} is the total energy of SWNT system. $E_{[EMI^+AlCl_4^-]}$ and $E_{[EMI^+Al_2Cl_7^-]}$ are calculated by optimizing the $EMI^+AlCl_4^-$ and $EMI^+Al_2Cl_7^-$, respectively as a molecular species due to non-availability of their crystal structures.

Therefore the average open circuit voltage (V_{ave}) for the system can be calculated as follows [28],

$$V = \left(\frac{\{{}^3/_x E_{[(AlCl_4)_xSWNT]} + 4E_{[EMI^+AlCl_4^-]} + E_{Al}\} - \{{}^3/_x E_{SWNT} + 4E_{[EMI^+Al_2Cl_7^-]}\}}{z}\right)$$

The average open circuit voltage calculated for (10,10), (15,15), (20,20) and (25,25) SWNTs are summarized in Table 1 and Figure S4 (Supporting Information). It can be seen that average

voltage increases with the increase of the tube diameter. For (25,25) SWNT, the cell voltage becomes 1.96 V which is close to the experimentally reported graphite system (2.00 V) [27, 32], and it can certainly improve for SWNTs with larger diameters leading to better performance in aluminium batteries.

Table 1: The average open-circuit voltage (V_{ave}), specific energy and specific capacity of different $AlCl_4$ adsorbed SWNT systems.

SWNTs	V_{ave} (V)	Specific Energy (eV)	Capacity (mAh/g)
(10,10)	1.70	1.76	223
(15,15)	1.76	1.86	236
(20,20)	1.80	1.97	251
(25,25)	1.96	2.14	275

To investigate the maximum capacity of different SWNTs, we calculated the specific energy of (10,10), (15,15), (20,20), and (25,25) SWNTs with $AlCl_4$ densities upto $(AlCl_4)C_{10}$, $(AlCl_4)C_{9.47}$, $(AlCl_4)C_{8.89}$, and $(AlCl_4)C_{8.11}$. The specific energy (E_S) is given by the following equation [71],

$$E_s = -(E_{SWNT+AlCl_4} - E_{SWNT})/m$$

where, $E_{CNT+AlCl_4}$ and E_{CNT} are the total energies of SWNT with and without $AlCl_4$, and m is the total number of carbon atoms in the supercell. The positive specific energy indicates that the system is stable and can accommodate m number of guest species. The calculated specific energy for each SWNT is given in Table 1. On the basis of the E_s value, we conclude that

(10,10), (15,15), (20,20) and (25,25) SWNTs stable up to $AlCl_4)C_{10}$, $(AlCl_4)C_{9.47}$, $(AlCl_4)C_{8.89}$, and $(AlCl_4)C_{8.11}$ unit formulas.

Therefore, based on the above unit formulas, we have further calculated the specific capacity using the following expression,

$$C = \frac{nxF}{M_f}$$

where, n is the number of electrons transferred per formula unit, x is the number of $AlCl_4$ molecules involved, F is the Faraday constant, and M_f is the mass of formula unit. The capacity calculated for each tube is listed in Table 1. The important point that can be inferred from this Table 1 and Figure S4 (Supporting Information) is about the variation of capacity with tube diameter. We have also shown how the adsorption energy, voltage and capacity vary on increasing the adsorption of $AlCl_4$ on (10,10) SWNT (Figure S5, Supporting Information). For (10,10) SWNT, the calculated capacity is 223 mAh/g, which further increases to 236 to 251 mAh/g for (15,15) and (20,20) SWNT respectively, and the specific capacity of as high as 275 mAh/g can be obtained with (25,25) SWNT. The systematic increase in capacity with increasing tube diameter is in accordance with the earlier studies on Li-ion batteries with SWNT electrodes.[68] The storage capacities obtained for the reported SWNTs are higher than that of the earlier studied graphite cathode (70 mAh/g) [27-29], which promotes the application of SWNTs as superior cathode host for aluminium batteries. Moreover, the level of theory (DFT-D3) used in our calculation is valuable enough to correlate with experimental studies [72] because the theoretical results of our previous study [28] on natural graphite have also been evaluated in a very recent experimental study [29, 32]. Therefore, we believe that a single-walled CNT with precisely large diameter will be able to offer the higher capacity and thus, will be suitable for practical applications.

Conclusions

In this work, we have investigated the potential applicability of a series of armchair single-walled carbon nanotubes (SWNTs) (5,5), (6,6), (10,10), (15,15), (20,20) and (25,25) for aluminium battery by studying the adsorption behaviour, electronic properties, average open-circuit voltages and storage capacities. It is demonstrated that the SWNTs can act as suitable cathode material for aluminium batteries. Through the structural studies, it is concluded that $AlCl_4$ adsorbs in its stable tetrahedral geometry and the AIMD study show that the $AlCl_4$ adsorbed SWNT system is stable at 300-600 K temperature range. The $AlCl_4$ prefers to adsorb at the hollow site above the centre of the hexagonal ring with the 3-Cl orientation. The studies show that for the small tubes the inner surface adsorption is more favourable than outer surface and inner centre adsorption and as the tube diameter increases the possibility of inner and outer surface adsorption becomes equal due to flattening of the tube and inner centre adsorption energy decrease due to increasing distance between tube surface and centre. The density of states calculations show the $AlCl_4$ adsorbed armchair SWNT system preserves its metallic nature, which is important for the electrode material. The charge density difference and Bader charge calculation indicate the oxidation of tube on $AlCl_4$ adsorption, showing a similar electrochemical behaviour as $AlCl_4$ intercalation into graphite. Moreover, our results show that SWNT shows very small diffusion barriers of 0.003 and 0.006 eV for $AlCl_4$ diffusion on inner and outer tube surface, respectively exhibiting excellent charge/discharge rates for aluminium battery. The average open-circuit voltages are in the range of 1.96 V which can further improve with the increase in diameter of SWNTs. In addition, our work reveals high specific capacities (more than 200 mAh/g) for SWNTs which increases with tube diameter and can be as high as 275 mAh/g in (25,25) tube, which is far better than the capacity of graphite cathode (70 mAh/g). Our findings

give a direction to explore carbon nanotube materials for aluminium batteries with large capacities, compatible voltages and high charge/discharge rates.

Computational Details

We have used the density functional theory (DFT) as implemented in the Vienna Ab initio Simulation Package (VASP) in all calculations [73-74]. The exchange-correlation potential is described by using the generalized gradient approximation of Perdew-Burke-Ernzerhof (GGA-PBE) [75]. The Projector augmented-wave (PAW) [76] method is employed to treat interactions between ion cores and valance electrons. The plane wave cut-off energy is fixed to 470 eV, which is sufficient for the convergence of total energy to 10^{-3} eV. The underlying structure optimizations are carried out using the van der Waals corrected density functional theory (DFT-D3) proposed by Grimme to overcome the deficiencies of DFT in treating dispersion interactions [72]. All the optimized structures are obtained by fully relaxing both atomic and lattice positions until the Hellmann-Feynman forces on all atoms are smaller than 10^{-3} eV/Å. During the relaxation, the Brillouin zone is represented by Monkhorst-Pack special k-point meshes of 1 × 1 × 6 for the SWNTs. To avoid the periodic image interaction between the SWNTs, the inter-tube distances are set to 25 Å and the supercells contain six layers of carbon atoms. The Bader charge analysis is performed to measure the charge transfer between $AlCl_4$ and SWNT [53-59]. The density of states calculations are carried out with 1 × 1 × 12 k-point sampling of Monkhorst-Pack grid. The diffusion barriers and the minimum energy paths for $AlCl_4$ hopping between two most stable adsorption sites are obtained by using climbing-image nudged elastic band method (CI-NEB) [77]. The minimum energy paths (MEPs) are initialized by considering six image structures between fully optimized initial and final structural geometries, and the energy convergence criteria of each image is set to 10^{-3} eV. Activation barriers are calculated by the

energy differences between the transition and initial states and the entropy corrections and Zero point energy (ZPE) correction are included while calculating the diffusion barriers. The ZPE is calculated as: ZPE $= \sum_i \frac{hv_i}{2}$, where h is Planck's constant and v_i is vibrational frequency. The ZPE of the system is calculated by considering only the degrees of freedom of intercalated $AlCl_4$.

Supporting Information

The supporting information file contents are relative energy values of different sites, adsorption energy plot for (10,10) SWNT, AIMD simulation analysis, optimized structures for all SWNTs with the respective diameters, adsorption energy and Bader charge analysis, variation of average open circuit voltage and specific capacity with increasing diameter of single-walled CNTs and variation of adsorption energy, voltage and storage capacity with increasing $AlCl_4$ adsorption on (10,10) SWNT.

Acknowledgments

We thank IIT Indore for the lab and computing facilities. This work is supported by DST-SERB, (Project Number: EMR/2015/002057) New Delhi. P.B. and A.M. thank MHRD for research fellowships.

References

1. M. S. Whittingham, MRS Bull. 33 (2008) 411-419.
2. J. Liu, J. G. Zhang, Z. Yang, J. P. Lemmon, C. Imhoff, G. L. Graff, L. Li, J. Hu, C. Wang, J. Xiao, G. Xia, Adv. Funct. Mater. 23(2013) 929-946.
3. M. Armand, J. M. Tarascon, Nature 451 (2008) 652−657.
4. R. V. Noorden, Nature 507 (2014) 26−28.
5. B. Dunn, H. Kamath, J. M. Tarascon, Science 334 (2011) 928-935.

6. J. B. Goodenough, K. S. Park, J. Am. Chem. Soc. 135 (2013) 1167-1176.

7. B. Scrosati, J. Hassoun, Y. K. Sun, Energy Environ. Sci. 4 (2011) 3287-3295.

8. B. L. Ellis, K. T. Lee, L. F. Nazar, Chem. Mater. 22 (2010) 691-714.

9. M. M. Thackeray, C. Wolverton, E. D. Isaacs, Energy Environ. Sci. 5 (2012) 7854-7863.

10. J. B. Goodenough, Y. Kim, Chem. Mater. 22 (2009) 587-603.

11. A. Manthiram, *J. Phys. Chem. Lett.,* 2 (2011) 176–184.

12. R. Mohtadi, F. Mizuno, Beilstein J. Nanotechnol 5 (2014) 1291-1311.

13. S. Rasul, S. Suzuki, S. Yamaguchi, M. Miyayama, Electrochim. Acta 82 (2012) 243-249.

14. M. M. Huie, D. C. Bock, E. S. Takeuchi, A. C. Marschilok, K. J. Takeuchi, Coord. Chem. Rev. 287 (2015) 15-27.

15. C. Xu, B. Li, H. Du, F. Kang, Angew. Chem. Int. Ed. 51 (2012) 933-935.

16. B. Lee, H. R. Lee, H. Kim, K. Y. Chung, B. W. Cho, S. H. Oh, Chem.Commun. 51 (2015) 9265-9268.

17. S. Liu, J. J. Hu, N. F. Yan, G. L. Pan, G. R. Li, X. P. Gao, Energy Environ. Sci. 5 (2012) 9743−9746.

18. L. Geng, G. Lv, X. Xing, J. Guo, Chem. Mater. 27 (2015) 4926−4929.

19. Q. Li, N. J. Bjerrum, J. Power Sources 110 (2002) 1−10.

20. N. S. Hudak, J. Phys. Chem. C 118 (2014) 5203−5215.

21. L. D. Reed, S. N. Ortiz, M. Xiong, E. J. Menke, Chem. Commun. 51 (2015) 14397−14400.

22. N. Jayaprakash, S. K. Das, L. A. Archer, Chem. Commun. 47 (2011) 12610−12612.

23. J. V. Rani, V. Kanakaiah, T. Dadmal, M. S. Rao, S. Bhavanarushi, J. Electrochem. Soc. 160 (2013) A1781−A1784.

24. P. R. Gifford, J. B. Palmisano, J. Electrochem. Soc. 135 (1988) 650−654.

25. S. Xia, X. M. Zhang, K. Huang, Y. L. Chen, Y. T. Wu, J. Electroanal. Chem. 757 (2015) 167−175.

26. M. Chiku, H. Takeda, S. Matsumura, E. Higuchi, H. Inoue, ACS Appl. Mater. Interfaces 7 (2015) 24385−24389.

27. M. C. Lin, M. Gong, B. Lu, Y. Wu, D. Y. Wang, M. Guan, M. Angell, C. Chen, J. Yang, B. J. Hwang, H. Dai, Nature 520 (2015) 324−328.

28. P. Bhauriyal, A. Mahata, B. Pathak, Phys. Chem. Chem. Phys. 19 (2017) 7980-7989

29. D. Y. Wang, C.Y. Wei, M. C. Lin, C. J. Pan, H. L. Chou, H. A. Chen, M. Gong, Y. Wu, C. Yuan, M. Angell, Y. J. Hsieh, Nature Commun. 8 (2017) 14283.

30. H. Sun, W. Wang, Z. Yu, Y. Yuan, S. Wang, S. Jiao, Chem. Commun. 51 (2015) 11892-11895.

31. Y. Song, S. Jiao, J. Tu, J. Wang, Y. Liu, H. Jiao, X. Mao, Z. Guo, D. J. Fray, J. Mater. Chem. A 5 (2017) 1282-1291.

32. K. V. Kravchyk, S. Wang, L. Piveteau, M. V. Kovalenko, Chem. Mater. (2017) DOI: 10.1021/acs.chemmater.7b01060.

33. G. Schmuelling, T..; Placke, R. Kloepsch, O. Fromm, H. W. Meyer, S. Passerini, M. Winter, J. Power Sources 239 (2013) 563-571.

34. T. Placke, S. Rothermel, O. Fromm, P. Meister, S. F. Lux, J. Huesker, H. W. Meyer, M. Winter, J. Electrochem. Soc. 160 (2013) A1979-A1991.

35. P. Bhauriyal, A. Mahata, B. Pathak, J. Phys. Chem. C. (2017) DOI: 10.1021/acs.jpcc.7b02290.

36. S. Iijima, Nature 56 (1991) 354-358.

37. D. A. Britz, A. N. Khlobystov, Chem. Soc. Rev. 35 (2006) 637-659.

38. S. M. Fatemi, M. Foroutan, Int. J. Environ. Sci. Technol. 13 (2016) 457-470.

39. Q. Zhao, M. B. Nardelli, J. Bernholc, Phys. Rev. B 65 (2002) 144105.

40. S. W. Lee, N. Yabuuchi, B. M. Gallant, S. Chen, B. S. Kim, P. T. Hammond, Y. Shao-Horn, Nature Nanotech. 5 (2010) 531-537.

41. B. Gao, C. Bower, J. D. Lorentzen, L. Fleming, A. Kleinhammes, X. P. Tang, L. E. Mcneil, Y. Wu, O. Zhou, Chem. Phys. Lett. 327 (2000) 69-75.

42. B. Gao, A. Kleinhammes, X. P. Tang, C. Bower, L. Fleming, Y. Wu, O. Zhou, Chem. Phys. Lett. 307 (1999) 153-157.

43. R. S. Morris, B. G. Dixon, T. Gennett, R. Raffaelle, M. J. Heben, J. Power Sources 138 (2004) 277-280.

44. S. H. Ng, J. Wang, Z. P. Guo, J. Chen, G. X. Wang, H. K. Liu, Electrochimica Acta 51 (2005) 23-28.

45. H. Shimoda, B. Gao, X. P. Tang, A. Kleinhammes, L. Fleming, Y. Wu, O. Zhou, Phys. Rev. Lett. 88 (2001) 015502.

46. E. Frackowiak, S. Gautier, H. Gaucher, S. Bonnamy, F. Beguin, Carbon, 37 (1999) 61-69.

47. G. Centi, S. Perathoner, ChemSusChem 4 (2011) 913-925.

48. S. Iijima, C. Brabec, A. Maiti, J. Bernholc, J. Chem. Phys. 104 (1996) 2089-2092.

49. A. A. Eliseev, L. V. Yashina, M. M. Brzhezinskaya, M. V. Chernysheva, M. V. Kharlamova, N. I. Verbitsky, A. V. Lukashin, N. A. Kiselev, A. S. Kumskov, R. M. Zakalyuhin, J. L. Hutchison, B. Freitag, A. S. Vinogradov, Carbon 48 (2010) 2708-2721.

50. H. Jiao, J. Wang, J. Tu, H. Lei, S. Jiao, Energy Technol. 4 (2016) 1112-1118.

51. S. Kumar, I. Choudhuri, B. Pathak, J. Mater. Chem. C 4 (2016) 9069-9077.

52. P. Garg, S. Kumar, I. Choudhuri, A. Mahata, B. Pathak, J. Phys. Chem. C 120 (2016) 7052-7060.

53. R. F. W. Bader, Chem. Rev. 91 (1991) 893−928.

54. G. Henkelman, A. Arnaldsson, H. Jónsson, Comput. Mater. Sci. 36 (2006) 354−360.

55. E. Sanville, S. D. Kenny, R. Smith and G. J. Henkelman, Comput. Chem. 28 (2007) 899−908.

56. W. Tang, E. Sanville, G. J. Henkelman, J. Phys.: Condens. Matter 21 (2009) 084204.

57. A. Mahata, P. Bhauriyal, K. S. Rawat, B. Pathak, ACS Energy Lett. 1 (2016) 797-805.

58. A. Mahata, K. S. Rawat, I. Choudhuri, B. Pathak, J. Mater. Chem. A 4 (2016) 12756-12767.

59. I. Choudhuri, S. Kumar, A. Mahata, K. S. Rawat, B. Pathak, Nanoscale 8 (2016) 14117-14126.

60. S. Kawasaki, T. Hara, Y. Iwai, Y. Suzuki, Mater. Lett. 62 (2008) 2917–2920.

61. G. Y. Sun, J. Kurti, M. Kertesz, R. H. Baughman, J. Phys. Chem. B 107 (2003) 6924-6931.

62. I. Cabria, J. W. Mintmire, C. T. White, Phys. Rev. B 67 (2003) 121406.

63. S. Gao, G. Shi, H. Fang, Nanoscale 8 (2016) 1451.

64. J. Kong, H. T. Soh, A. M. Cassell, C. F. Quate, H. Dai, Nature 395 (1998) 878-881.

65. N. P. Stadie, S. Wang, K. V. Kravchyk, M. V. Kovalenko, ACS Nano 11 (2017) 1911-1919.

66. G. Martyna, M. Tuckerman, D. Tobias, M. Klein, Mol. Phys. 87 (1996) 1117-1157.

67. S. Takahashi, N. Koura, S. Kohara, M. L. Saboungi and L. A. Curtiss, Plasmas Ions 2 (1999) 91.

68. M. Zhao, Y. Xia, L. Mei, Phys. Rev. B 71 (2005) 165413.

69. M. K. Aydinol, A. F. Kohan, G. Ceder, K. C. Joannopoulos, J. Phys. Rev. B 56 (1997) 1354.

70. M. K. Aydinol, A. F. Kohan, G. Ceder, J. Power Sources 68 (1997) 664-668.

71. P. Larsson, R. Ahuja, A. Nyten, J. O. Thomas, Electrochem. Commun. 8 (2006) 797−800.

72. S. Grimme, J. Antony, S. Ehrlich, H. Krieg, J. Chem. Phys. 132 (2010) 154104.

73. Y. Chen, F. Peng, Y. Yan, Z. Wang, C. Sun, Y. Ma, J. Phys. Chem. C 117 (2013) 13879-13886.

74. G. Kresse, Furthm¨uller, J. Phys. Rev. B: Condens. Matter Mater. Phys. 54 (1996) 11169–11186.

75. P. E. Blöchl, Phys. Rev. B 50 (1994) 17953.

76. J. P. Perdew, K. Burke, M. Ernzerhof, Phys. Rev. Lett. 77 (1996) 3865-3868.

77. G. Mills, H. Jónsson, G. K. Schenter, Surf. Sci. 324 (1995) 305-337.

10.1002/asia.201700570

Table of Content:

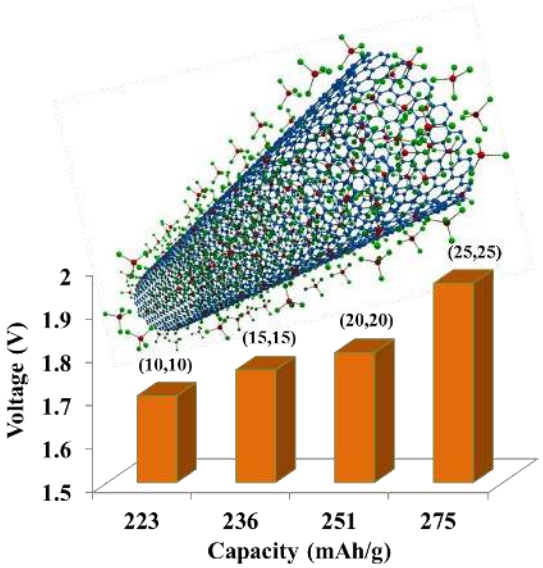

Variation of Voltage and Capacity with the tube diameter for armchair single-walled carbon nanotubes